Pharmaceutical Research, Vol. 25, No. 11, November 2008 (© 2008)
DOI: 10.1007/s11095-008-9660-x

Research Paper

Design of a Device for Simultaneous Particle Size and Electrostatic Charge Measurement of Inhalation Drugs

Kewu Zhu,[1,4] Wai Kiong Ng,[1] Shoucang Shen,[1] Reginald B. H. Tan,[1,2] and Paul W. S. Heng[3]

Received April 4, 2008; accepted June 9, 2008; published online July 1, 2008

Purpose. To develop a device for simultaneous measurement of particle aerodynamic diameter and electrostatic charge of inhalation aerosols.
Method. An integrated system consisting of an add-on charge measurement device and a liquid impinger was developed to simultaneously determine particle aerodynamic diameter and electrostatic charge. The accuracy in charge measurement and fine particle fraction characterization of the new system was evaluated. The integrated system was then applied to analyze the electrostatic charges of a DPI formulation composed of salbutamol sulphate-Inhalac 230® dispersed using a Rotahaler®.
Results. The charge measurement accuracy was comparable with the Faraday cage method, and incorporation of the charge measurement module had no effect on the performance of the liquid impinger. Salbutamol sulphate carried negative charges while the net charge of Inhalac 230® and un-dispersed salbutamol sulphate was found to be positive after being aerosolized from the inhaler. The instantaneous current signal was strong with small noise to signal ratio, and good reproducibility of charge to mass ratio was obtained for the DPI system investigated.
Conclusions. A system for simultaneously measuring particle aerodynamic diameter and aerosol electrostatic charges has been developed, and the system provides a non-intrusive and reliable electrostatic charge characterization method for inhalation dosage forms.

KEY WORDS: aerosol; aerosolization; device; electrostatic charge; inhalation drug delivery.

INTRODUCTION

Determination of particle electrostatic charges and diameters is important to certain problems related to the monitoring indoor and outdoor environment, the inhalation drug delivery to the lung, as well as the processing and handling of industrial powders. In the chemical and pharmaceutical industries, particle electrification has been associated with solid handling processes such as in the powder pneumatic conveying (1–3), gas–solid fluidized bed (4–5), melt agglomeration process (6), powder blending (7), and spry drying process (8). Electrostatic charges can greatly alter the particle flow dynamics, and hence the system performance.

Electrification of aerosol particles in dry powder inhaler (DPI) and metered dose inhaler (MDI) has recently emerged as an important subject in the pulmonary drug delivery research as electrostatic charges have been shown to influence the efficiency of pulmonary drug delivery by their effects on powder adhesion or retention on inhalers, deaggregation of drug from carrier particles, and lung deposition of the active drug particles (9–11). In the formulation of dry powder inhalation products, mixing is regarded as a key process for preparing fine drug particles with coarse carrier particles to form a homogeneous mixture. Electrostatic charges were found to be generated and accumulated as a result of continuous collisions between the particle and the wall of mixer container as well as between particles, which affected binding between the particle and the container wall as well as between particles and hence influenced the quality of final products (12). These electrostatic charges, if not dissipated, were shown to enhance the inter-particle interaction forces leading to a reduction in the dose of delivered medications (13–15). In addition, electrostatic charges were reported to be generated during aerosolization processes as well (9–10). These electrostatic charges were shown to not only influence the motion of drugs in the respiratory tract but also the deposition of aerosol particles in the lungs (16,17), and therefore the therapeutic effect. Knowing the importance of electrostatic charges in the inhalation drug delivery systems (14,18–20), many researchers have investigated various aspects of electrostatics in the pulmonary drug delivery systems. Electrostatic charges carried by aerosols in the pulmonary drug delivery systems were characterized (11,21). Carrier property (8), device material (22), and environmental condition during storage or aerosolization processes (14–15) were all reported to have important influences on the electrostatic charges of the aerosols. In spite of its importance in the

[1] Institute of Chemical and Engineering Sciences, A*STAR (Agency for Science, Technology and Research), 1, Pesek Road, Jurong Island, Singapore 627833, Singapore.
[2] Department of Chemical & Biomolecular Engineering, National University of Singapore, 4 Engineering Drive 4, Singapore 117576, Singapore.
[3] Department of Pharmacy, National University of Singapore, 18 Science Drive 4, Singapore 117543, Singapore.
[4] To whom correspondence should be addressed. (e-mail: Zhu_Kewu@ices.a-star.edu.sg)

pulmonary drug delivery, our understanding on the electrostatic charge is still limited.

Particle size is one of the key parameters for inhalation drug delivery. To be effective for the pulmonary drug delivery, particles should have a narrow size distribution ranging from 1 to 5 μm (23). The aerodynamic diameter distribution is normally determined using an inertia impactor (24). Recognizing the importance of particle size and electrostatic property of inhalation aerosols, devices that allow simultaneous measurement of these two properties are of great importance. Electrostatic charges could be measured using a direct method such as a Faraday cage method. Charged particles were introduced into a Faraday cage and the total or net charges were measured. The charge to mass ratio was then calculated if the mass introduced into the Faraday cage was known. However, no information on the relation between electrostatic charge and particle size can be determined using this method alone. In addition to direct charge measurement techniques, electrical mobility analyzer (25–26) and Electric Single Particle Aerodynamic Relaxation Time (E-SPART) (27–28) employed indirect measurement techniques to determine the electrostatic charges on particles. In the electrical mobility analyzer, the particle was exposed to an electrical field while particle motion in response to the field was monitored optically or by other means. The average size and charge could be found from the deflection of the particle. However, particles larger than a few micrometers are not easily handled by electrical mobility analyzers, which require relatively high electric fields. E-SPART acquired images of tracks of aerosol particles falling through an oscillating electric field, located pixels in each image that formed the individual tracks, and created non linear curve fits of the tracks in order to determine track parameters. These parameters were then used to estimate the size and charge of each particle. However, this device may be physically very large and costly to build. Electrical Low Pressure Impactor (ELPI) (29), primarily designed for particle sizing through the combination of electrical detection and impaction collection, has been recently explored for charge measurement of inhalation powders (14,21,30,31). Operating at 30 LPM and a maximum cutting size of about 10 μm, ELPI without modification may not be applicable for dry powder inhaler testing which normally operates at 60 LPM, and cannot be used to characterize electrostatic charges of carrier particles that are normally of about a few tens of microns.

There is a need to have a simple device that can dynamically measure electrostatic charges and aerodynamic diameters simultaneously of drug particles. To be effective, the device should be able to operate over a wide air flow range, at a high sampling rate, and over a wide range of particle sizes. The purpose of this study is to develop a system for measuring electrostatic charge and particle aerodynamic diameter simultaneously during aerosolization. The new system is composed of a liquid impinger with which particle aerodynamic diameters were measured and an independent add-on device to non-intrusively measure electrostatic charges simultaneously. A Twin Stage Impinger (TSI) was chosen in the current study as an illustration, although the same measuring principle can be applied to other impingers. The new system can accept any size range and air flow condition that the liquid impinger can operate. In the current study, the TSI can be operated from 30 to 90 LPM and larger carrier particles of several tens micron are separated at upper stage. And the sample frequency is also much higher, for example, in the current work the sampling frequency used was 100 HZ. The accuracy of the electrostatic charge measurement of the new system was evaluated using the Faraday cage method. Effects of the incorporation of the add-on device and change of collection liquid on the performance of the TSI were evaluated with respect to the fine particle fraction (FPF). The reliability in the charge to mass ratio measurement of the device was illustrated using the model DPI system. The device developed may be useful in the inhalation drug delivery research.

MATERIALS AND METHODS

Materials

Two grades of lactose monohydrate, namely Inhalac 230® and Sorbalac 400® (Meggle, Germany), were used. Inhalac 230® was sieved to 63 to 90 μm size fraction using a jet sieve (Hosokawa Micron, USA) under vacuum pressure of 20–25 cm water for 120 s. Sorbalac 400® was used as supplied. Salbutamol sulphate, purchased from JunDa Pharma (ChangZhou, PRC), was micronized to 1–5 μm using an air jet mill. These particles were sealed in a glass bottle and stored in a desiccator over silica gel at room temperature until further required. Throughout the investigation, high purity water produced by the reverse osmosis (MilliQ, Millpore, France) was used.

Particle Characterization

Particle size distributions were measured with a laser diffraction technique with the wet dispersion mode using Malvern Mastersizer 2000 (Malvern Instruments, UK). Butan-1-ol and cyclohexane were used as the dispersion media for lactose monohydrate and salbutamol sulphate respectively. Before each measurement, the sample was sonicated for about 30 s. The aerodynamic diameter distribution was determined using the Aerosizer PSD 3603 (TSI Incorporated, US). A small amount of powder (about 5 mg) was placed in the sample cup of the aerosol disperser. Particle size distribution measurement was carried out at the predetermined air flow rate and using the 100% sample feeding mode. Time-of-flight (TOF) data were processed with the operating software package (TSI Incorporated, US) and the true particle densities of Inhalac 230®, and Sorbalac 400® and salbutamol sulphate at 1.53, 1.52, and 1.32 g/ml respectively, which were measured using Ultrapcynometer 1000 (Quantachrome, USA). Both the number- and volume-based particle size distributions (PSD) were obtained. All PSD measurements were done in triplicate to ensure reproducibility. Bulk particle density was determined using autotap density meter (Quantachrome, USA).

Blend Preparation and Uniformity Testing

Milled salbutamol sulphate (0.75 g) and 14.25 g sieved Inhalac 230® (63–90 μm) were blended in a glass bottle using a T2F Turbula mixer (Switzerland) at 49 rpm for 30 min. Content uniformity of blends was ascertained by withdrawing 5 samples from different locations in the powder bed. Four of

them were taken at locations evenly distributed around the bottle wall, and the fifth sample was taken from the center. The sample was weighed and dissolved in water for HPLC analysis according to the method described in the following section.

HPLC Analysis of Salbutamol Sulphate

Salbutamol sulphate content was analyzed using HPLC with a mixture of 5.4% (*w*/*v*) sodium acetate anhydrous and 2.4% (*w*/*v*) acetic acid as the mobile phase at the flow rate of 1 ml/min and a UV detector at the wavelength of 276 nm. A 15 cm×4.6 mm i.d. column packed with 3.5 μm C-18 was used throughout the measurements. The measured retention time for salbutamol sulphate was approximately 2.6 min. Standard solutions were prepared for drug concentrations ranging from 0.1 to 15 μg/ml, in order to construct a calibration curve of drug concentration against the peak area. The calibration was considered to be acceptable when R^2>99.99%.

Capsule Filling and Storage

Hard gelatin capsules (#3) were manually filled with 20± 1 mg of the binary mixture. Twenty filled capsules were placed in a labelled bottle stored inside an environmental chamber (Model 518, ETS, USA) at 20% relative humidity and 25°C for 24 h prior to *in vitro* analysis.

In vitro Study

In vitro analysis of the formulation was performed with a TSI (Copley Scientific, Nottingham, UK) using the method according to the British Pharmacopoeia. Seven and 30 ml of appropriate solvents were introduced in the stages I and II of the TSI respectively. A filled capsule was inserted into the Rotahaler® (GlaxoSmithKline, Ware, UK), and the cap and body of the capsule were separated after rotating the cap of Rotahaler®. The Rotahaler® was then mounted to a specially built mouthpiece adapter. Before switching on the vacuum pump, the assembly was firstly checked for air tightness. The test was performed for 5 s at the pump air flow rate of 60 LPM, which was verified prior to the test using a digital flow meter (Copley Scientific, UK). The capsule shells were removed from the inhaler device after testing. The deposition test was carried out for 20 capsules with the method just described. The drug fractions retained at DPI, coated at the glass throat, and deposited at both stages of TSI were collected by washing with water five times. These collected solutions were then made up to 250 ml, and the concentrations of salbutamol sulphate in these solutions were analyzed using HPLC. All the measurements were carried out at the pre-selected RH and at 25°C inside a walk-in environmental chamber.

Charge Measurements

Figure 1 shows the schematic diagram of the experimental setup. In the present study, a glass type twin-stage impinger (TSI) was used to as an illustration. The principle, however, could be well applied to other multi-stage impingers. The TSI, composing of throat (2), stage 1 (3), stage 2 (4) including the second impinging tube, was connected to a vacuum pump (7) via a control valve (5) and

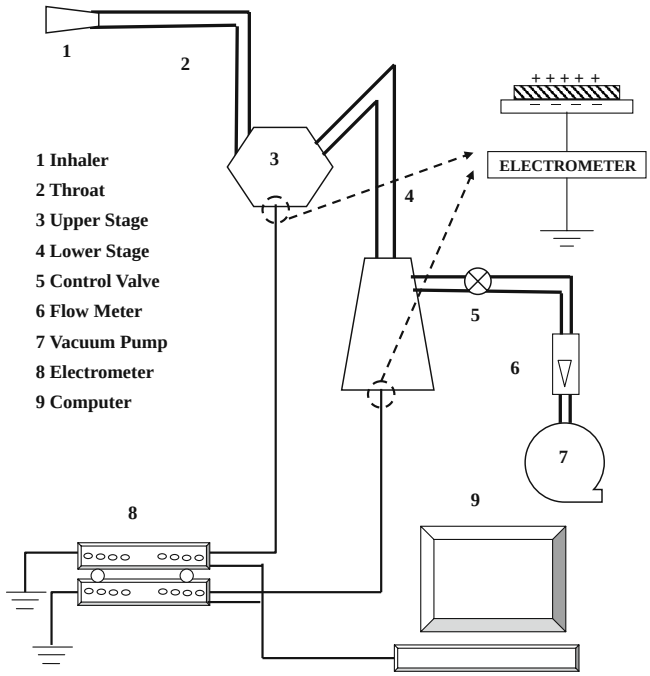

Fig. 1. Schematic diagram of the experimental setup.

a flow meter (6). Two sensors were installed on the outside of the bottom wall of both stages 1 and 2 of TSI. Upon aerosolization at specific velocity, particles were deposited at either stage 1 or 2 depending on their aerodynamic diameters. If particles were charged, the same amount of charges would be induced at these two electrodes upon particle deposition. The rate of induction charge build-up was measured as induction current by connecting the electrodes to the ground via a charge sensitive amplifier (8), for example, electrometers, and recorded by a computer (9). An independent method, the Faraday cage method, was used to measure the particle charges after aerosolization to ensure the accuracy of charge measurement with the proposed method using Inhalac 230®, Sorbalac 400®, and salbutamol sulphate particles that were stored in a silica filled dessicator for at least 48 h prior to measurements.

Add-on Device and Solvent Effects

It is very crucial to learn whether the installation of the charge measurement system or the change of collection liquid will affect the performance of the TSI with respect to the characterization of the DPI drug delivery system. This was done through a series of experiments employing a two-factor and two-level full factorial experiment design method. The two factors were the add-on device and the solvent type. Dummy factor was employed according to following: "−1" refers to no add-on device was installed or the collection liquid was water, and "1" refers to the add-on device was installed and activated during TSI operating process, or the solvent was silica oil. The full factorial two-factor and two-level design yielded four experiments. To examine the experimental reproducibility, three extra tests were carried out for the setup using silica oil as the collection solvent and with the charge measurement system installed and activated.

Statistics

Statistical analysis was performed for electrostatic charge measurements. To evaluate the accuracy of the current method against the faraday cage method, F test and t test were employed to evaluate whether these two methods were significantly different. One-way ANOVA test was used to analyze the reproducibility using three independent measurements on the electrostatic charges at upper/lower stages of 20 actuations. The significance level was specified at $p<0.05$.

THEORETICAL

In the present study, the add-on device was designed and incorporated with a standard liquid impinger to simultaneously measure particle charges and aerodynamic diameters of inhalation particles. Particles can be separated into different size fractions upon passing through the liquid impinger according to their inertia. The operational principles of the liquid impinger are well known and can be found elsewhere (24,32). Compared to normal cascade impactors, liquid impingers use liquid to collect particles upon their inertia impaction. The use of liquid for collection overcomes the problems of particle re-bounce and inter-stage loss, commonly present in normal cascade impactors. Upon deposition of particles on the surface of the collection vessel, the electrostatic charges carried by the particle can be detected via the charge induction method through the electrode attached to the bottom of the particle collection vessel.

When particles are deposited at the dielectric collection vessel from the inhalation air stream, the corresponding electrostatic charges carried by these particles will be taken by the layer of collection liquid. The amount of the charge accumulated at the layer of collection liquid depends on the number of particles collected, the amount of electrostatic charges carried by each particle, and the amount of charge dissipated, which can be expressed as:

$$Q = \sum_{p=1}^{N} q_p - Q_d \tag{1}$$

Where,

Q is the total amount of charges trapped in the collection liquid due to particle deposition;
N is the total number of particles deposited;
q_p is the charge carried by particle p;
Q_d is the amount of charge dissipated.

When an electrode is installed at the bottom wall of the collection vessel, an equal amount of charge will be induced at the electrode. The amount of charge can be detected through a charge sensitive amplifier. During inhalation tests, many particles continuously impact and deposit in the collection liquid. The charge accumulation rate in the collection liquid can be evaluated using the induction current, $i_{ind,}$ which is obtained by differentiating equation (1) with time:

$$i_{\text{ind}} = \frac{dQ}{dt} = \frac{d}{dt}\left(\sum_{p=1}^{N} q_p\right) - \frac{dQ_d}{dt} \tag{2}$$

If the charge dissipation rate is low, the induction current can be approximated to the accumulation rate of electrostatic charges at the particle collection vessel as follows:

$$i_{\text{ind}} = \frac{dQ}{dt} \cong \frac{d}{dt}\left(\sum_{p=1}^{N} q_p\right) \tag{3}$$

By installing the charge measurement devices to the various stages of the multi-stage impinger, induction currents associated with particle deposition at the various stages can be determined according to the method just described. Integration of this add-on device with the multi-stage impinger can then give valuable information on both the particle aerodynamic diameters and aerosol electrostatic charges.

As the transient induction current is measured, both the magnitude and polarity of the electrostatic charge can be detected dynamically. Provided that the temporal resolution is high enough, the current method may also detect bipolar charge distributions.

The charge profile of aerosols is obtained through integration of the induction current over detection time. The profile of the electrostatic charge can provide valuable information on how drug particles are emitted from the inhaler, which may be used to evaluate the emission behaviour of the drug formulation and inhaler design. Using either a weighing or chemical analysis method, the mass of particles deposited at various stages can be obtained, and the charge to mass ratio of various size fractions can be calculated in a straightforward manner.

RESULTS AND DISCUSSION

Particle Characterization

The particle physical properties of Inhalac 230®, Sorbalac 400® and salbutamol sulphate were summarized in Table I. The tapping densities were 0.37, 0.65, and 1.04 g/ml and the volume mean particle diameter were 4.06, 8.41, and 80.21 μm for salbutamol sulphate, Sorbalac 400®, and Inhalac 230® respectively. Compared to Inhalac 230® particle, salbutamol sulphate and Sorbalac 400® particles had smaller tapping densities. The loose packing of salbutamol sulphate and Sorbalac 400® particles was probably due to their cohesive characteristics.

Table I. Physical Property Salbutamol Sulphate, Sorbalac 400®, and Inhalac 230®

Material	Tapping density[a] (g/ml)	True density[b] (g/ml)	Mean diameter[c] (μm)
Salbutamol sulphate	0.37	1.32	4.06
Inhalac 230®	1.04	1.53	80.21
Sorbalac 400®	0.65	1.52	8.41

[a] Tapping density was measured using an autotap density meter (Quantachrome, USA).
[b] True density was determined using a Ultrapycnometer 1000 system (Quantachrome, USA).
[c] Mean diameter was characterized using a particle size distribution analyzer via time-of-flight technique (PSD 3603, TSI, USA).

Table II. Validation of the Charge Measurement of the Add-on Device Against the Faraday Cage Method at the Same Environmental Conditions: 25°C and 20% RH

Materials	Present method (nC/g)	Faraday cage method (nC/g)	Difference%
Inhalac 230®	−82.4±11.4	−87.3±6.3	5.6
Sorbalac 400®	−137.2±27.3	−104.6±17.5	31.2
Salbutamol Sulphate	−442.9±85.7	−348.0±54.7	27.3

System Evaluation

Add-on Device Charge Measurement Evaluation

The accuracy of the charge measurements using the add-on device was ascertained against the Faraday cage method. Table II compares the results of electrostatic charge measurements by the proposed method with those by the Faraday cage method for salbutamol sulphate, Sorbalac 400®, and Inhalac 230® particles, respectively. The charge to mass ratios measured by the proposed method were found to be −82.4± 11.4, −137.2±27.3, and −442.9±85.7 nC/g for Inhalac 230®, Sorbalac 400® and salbutamol sulphate respectively. The corresponding charge to mass ratios characterized using the Faraday cage method were −87.3±6.3, −104.6±17.5, −348.0± 54.7 nC/g. The difference between these two measurement methods were 5.6%, 31.2%, and 27.3% for Inhalac 230®, Sorbalac 400®, and salbutamol sulphate respectively.

The variations in the particle electrostatic charges measured employing the Faraday cage method are commonly found to be about several tens percent. For example, Elajnaf *et al.* (33) reported the covariance of charge to mass ratio for five measurements using Faraday cage was about 50% in some cases in their investigation on the effect of contact surface and relative humidity on particle charge accumulation and adhesion of powders used for inhalation from DPIs. Telko *et al.* (30) also found that the covariance of at least three repetitive measurements using ELPI was about 50% in some cases in their characterization of the electrostatic charges of aerosols delivered by dry powder inhalers. In the present study, the differences in the charge to mass ratios measured using the proposed add-on device and the Faraday cage method were well within the variance range of repeated measurements using the Faraday cage method reported in the literature, which suggests that the accuracy of the proposed add-on device is comparable to the Faraday cage method. Comparing the current method to the faraday cage method, t-Test (95% confidence level) indicated no significant difference in precision and *F* test (95% confidence level) suggested no significant difference in accuracy.

Effect of Add-on Device and Collection Solvent

The coded experimental design matrix together with the experimental results is shown in Table III. The order of testing was carried out randomly. A generalized linear model was used to evaluate the significance of the two factors. The linear regression equation was $\tilde{y} = 8.2 + 0.17 \times x_1 + 1.5 \times 10^{-3} \times x_2$. The replicate and lack-of-fit errors were 0.18 and 1.1×10^{-2} respectively. The ratio of lack-of-fit to the replicate errors was found to be about 0.06, which indicated that the model prediction error was negligible compared to the experimental errors. The variations in the fine particle fractions arising from the change of collection solvent from water to silica oil and/or the installation of add-on device were therefore not greater than the experimental errors, which suggested that the two factors had negligible effects on the performance of the TSI with respect to the fine particle fraction characterization.

CHARACTERIZATION OF THE BINARY FORMULATION

Induction Current Profile

The cutting size of the TSI at the current testing condition (60 LPM) was 6.4 μm. Therefore the materials deposited at the upper stage were inhalac 230® and the undispersed salbutamol sulphate, while those deposited at lower stage were salbutamol sulphate. Electrostatic charges, introduced to the collection solvent accompanying the particle deposition, would induce the same amount electrostatic charges of opposite polarity at the detection sensors (34). Therefore induction current of the same polarity as the electrostatic charges carried by the deposited particles would flow to the ground through the detection sensors, and the electrostatic charges can be evaluated through integration of the induction current over time. The current profile could provide information on the deposition pattern of the particles. The typical induction current profile is shown in Fig. 2A. The solid line shows the signal from first stage (upper stage) of TSI which measures the charge accumulation rate associated with the deposition of lactose carrier and un-dispersed salbutamol sulphate particles. The broken line is the signal from second stage (lower stage) of TSI which reflects the rate of charge trapped due to the deposition of salbutamol sulphate drug particles. As shown in the figure, both signals were very strong with small noise to signal ratios. The current profiles probably reflected the particle deposition pattern provided the electro-

Table III. Effect of Solvent/charge Measurement on the Performance of TSI

Testing	Factor 1	Factor 2	Response
1	−1	−1	8.42
2	−1	1	7.58
3	1	−1	8.01
4	1	1	7.87
5	1	1	8.2
6	1	1	8.55
7	1	1	8.36

Factor 1 Solvent type (*−1* water, *1* silica oil); *Factor 2* using charge measurement system? (*No* −1, *Yes* 1); *Response* fine particle fraction, %

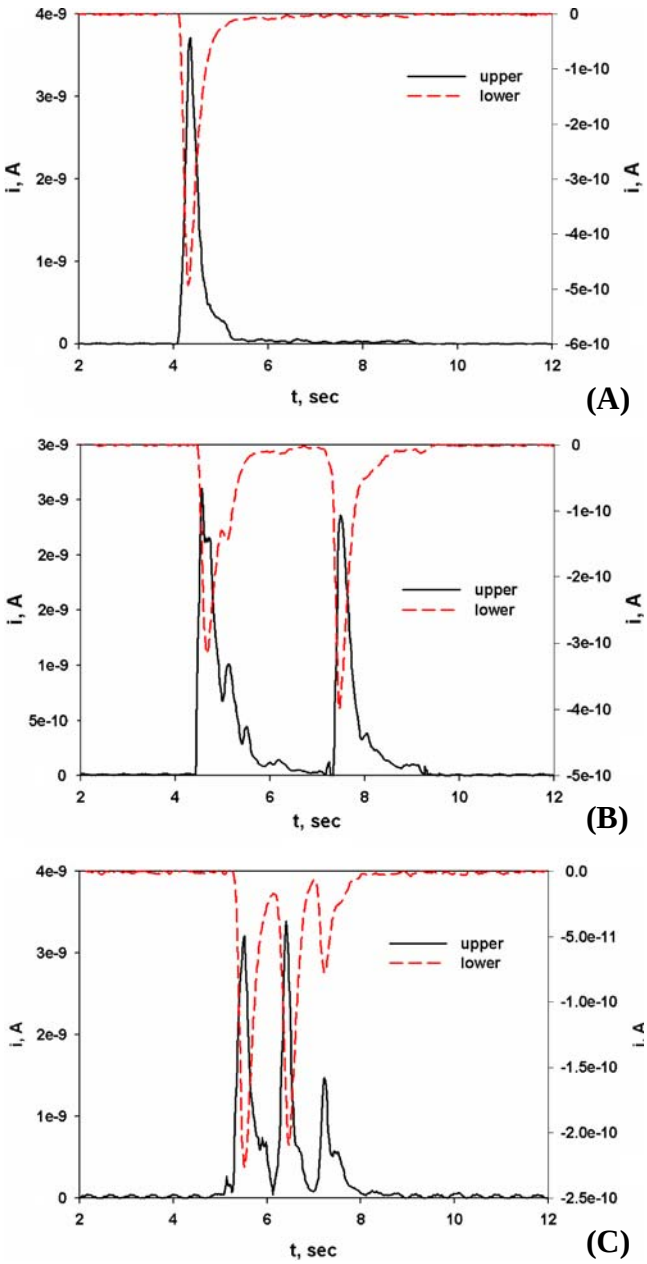

Fig. 2. Induction current profiles measured at the upper and lower stage of Twin Stage Impinger for single actuation. *Solid line* Upper stage; *dashed line* lower stage. **A** One-pulse profile; **B** double-pulse profile; **C** triple-pulse profile.

static charges were uniformly distributed over particles. The sharp peaks in the induction current profiles indicated that the deposition of the particles was in impulse fashion, and it was clearly shown that the duration for the particle pulse to deposit at the respective stage was less than 2 s. Apparently, the net charge of particles deposited in the first stage was positive, and that of particles deposited at the second stage was negative. The negative charge polarity of salbutamol sulphate is in agreement with previous studies which have reported that the salbutmol sulphate carried negative charges when dispersed from a lactose carrier based formulation (9,14). The magnitude of net charges associated with particles on the first stage was almost one order larger than that on the second stage. Lactose carrier and drug particles carried electrostatic charges with opposite polarity, which enhanced the particle adhesion force and may lead to poor aerosol dispersion efficiency.

In addition to the impulse in the current profile described above, two-pulse (Fig. 2B) and three-pulse (Fig. 2C) current profiles were also observed in the current study. These multiple peaks in the current profiles were unlikely due to some disturbance from the measurement system because multi-peak signals from both first and second stages were almost simultaneously detected. The double- and/or triple-distinct pulses in the current profiles suggest the discontinuous release of the formulation in the pulse fashion. The total charge for the two-pulse profile shown in Fig. 2B was 2.38 and −0.32 nC for the first and second stages respectively. And the corresponding electrostatic charges for the first and second stages of the triple-pulse profile shown in Fig. 2C was 2.54 and −0.18 nC. The total charges for the two-pulse and three-pulse current profile were in the same order as those of single pulse current profiles, for example, the net charge of single pulse profile shown in Fig. 2A was 1.75 and −0.19 nC for the first and second stages respectively. The time evolution of the current profile can provide important information on the formulation release profile from the inhalers, which might be useful for optimization of the drug formulation and/or inhalation device design.

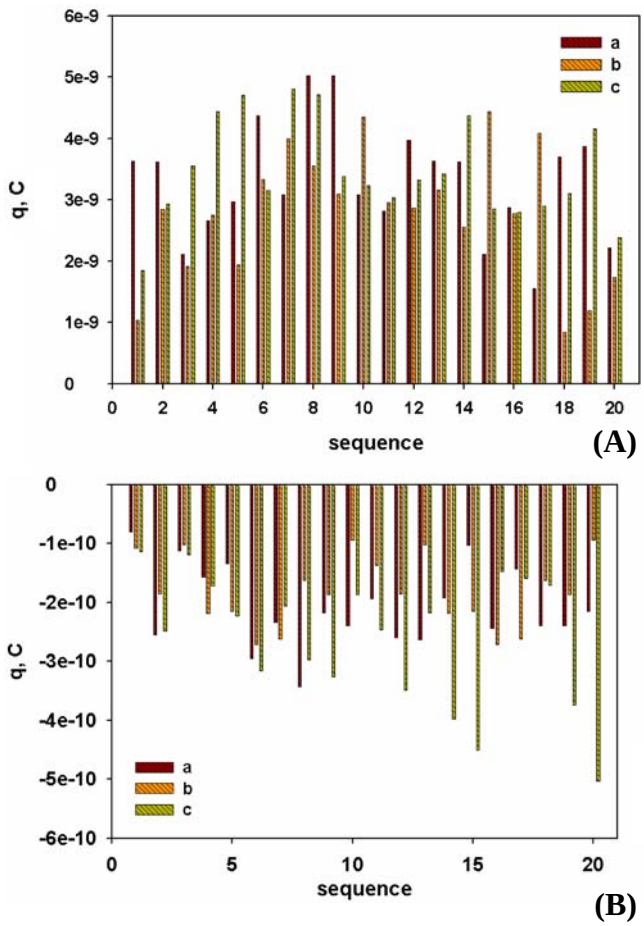

Fig. 3. Electrostatic charge characterization results using the proposed method for three independent tests composed of 20 actuations each at 25°C and 20% RH. **A** Upper stage; **B** lower stage.

Table IV. Summary of the Charge to Mass Ratio Measurements of the Inhalation Drugs Using the Proposed Method upon Aerosolization of the Salbutamol Sulphate-lactose Formulation from the Rotahaler®

	Q (nC)		*CV* (~) %			
Tests	Upper	Lower	Upper	Lower	Mass of SS (mg)	Q/M (μC/g)
A	66.6	−4.12	28.3	32.8	1.02	−4.04
B	55.4	−3.54	38.5	33.4	1.06	−3.34
C	69.2	−5.22	23.8	42.7	1.11	−4.70
Average					1.06	−4.03
STD					0.05	0.68
CV %					4.24	16.9

Testing was performed under walk-in chamber at 25°C and 20% RH.

Electrostatic Charge Measurement

The net electrostatic charge of particles deposited in each stage during each actuation was obtained by integrating the induction current over inhalation time. This was done automatically using an in-house program written in MatLab. Three tests, each composing of 20 actuations, were performed at the same conditions but different days to evaluate the test to test and actuation to actuation variations in the electrostatic charge measurements.

Figure 3 shows the electrostatic charges associated with particles deposited in the first (Fig. 3A) and second (Fig. 3B) stages for 20 actuations of the three different tests. The three tests were performed on three different days in the walk-in environmental chamber at the temperature of 25°C and the relative humidity of 20%. There was no clear trend on the dependence of the charge on the inhalation test sequence although effect of repeated use of inhaler on the charge measurement results was reported in literature (9). As no effort was made for optimizing the performance of the inhaler and/or the formulation, it was likely that the delivered dose might vary a bit from actuation to actuation, which contributed to the variation of electrostatic charge of each actuation. Therefore the variation in electrostatic charge from actuation to actuation could arise from the variation in delivered dose and/or the effect of inhaler. In the upper stage, the net electrostatic charges of deposited particles were ranged from 1.55 to 5.03 nC, 0.85 to 4.44 nC, and 1.85 to 4.81 nC for the testing a, b, and c respectively. The corresponding coefficients of actuation to actuation variations in the electrostatic charge were 28.3%, 38.5%, and 23.8%. For the lower stage, the net electrostatic charges of deposited particles were ranged from −80 to −343 pC, −94 to −272 pC, and −113 to −503 pC with the corresponding coefficients of actuation to actuation variations in the electrostatic charges of 32.8%, 33.4%, and 42.7% for the testing a, b, and c respectively. ANOVA analysis (95% confidence level) indicated that the three independent measurements were not significantly different.

The average electrostatic charges per actuation of the total 20 actuations were 3.33, 2.77, and 3.46 nC for the first stage and −0.21, −0.18, and −0.26 nC for the second stage for the three tests a, b, and c respectively. The mean electrostatic charges of the three tests were 3.18 and −0.22 nC for the first and second stages respectively, and the corresponding coefficient of variation for the three tests were found to be 11.4% and 18.6%.

The results of charge measurements are summarized in the Table IV. The mass of salbutamol sulphate deposited in the second stage were analyzed by the HPLC method described earlier and were 1.02, 1.06, and 1.11 mg for the total 20 actuations of testing a, b, and c respectively. The average mass for the three tests was 1.06 mg with the coefficient of variations of 4.24%. The small coefficient of variation indicated good experimental reproducibility with respect to the fine particle dose. Dividing the net electrostatic charges by the corresponding mass of particles, the charge to mass ratios of the three tests were found to be −4.04, −3.34, −4.70 μC/g for test a, b, and c respectively, which led to the mean charge to mass ratio of −4.03 μC/g and the coefficient of variance of 16.9%.

The results indicated that, using the proposed add-on device, actuation to actuation and testing to testing variations in electrostatic charge measurement were reasonably small, which suggested that electrostatic charge measurements using the proposed method were reliable and consistent for the DPI system investigated.

DISCUSSION

In the current study, the principle and method to measure the electrostatic charges of inhalation drug particles were illustrated using the twin-stage impinger. The same principle and method can also be extended to particle charge characterization in general. For example, milled particles can be

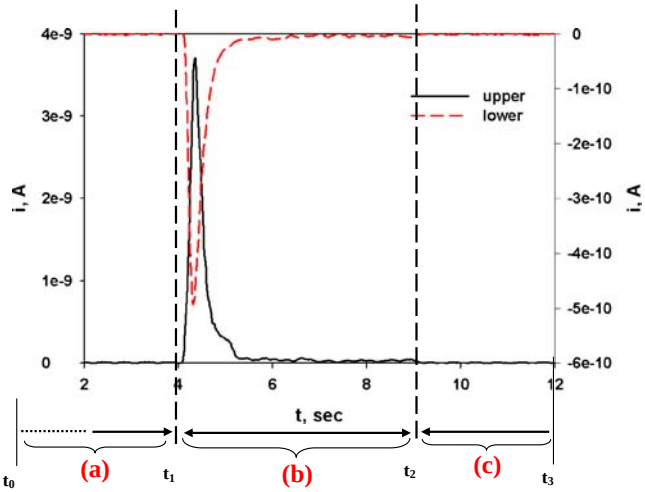

Fig. 4. Electrostatic charge measurement procedures. *a* Measurement of current before formulation testing; *b* measurement of induced current from the deposited particles; *c* measurement of current after formulation testing.

directed into single liquid particle trapping system so that the effect of milling on the particle electrification can be studied. Other applications include particle electrification in process equipments. Particles can be directed through a tube made of the same material as the equipment and collected in a single stage, where the particle charges can be measured using the current method and particle electrification can be investigated.

One concern of the present charge measurement method is about the influence of residual charges from previous measurements. In the present device, the charge was measured through the induction current. It is true that the residual charge of previous measurements will distort current measurement, and this distortion, mainly due to the charge dissipation, is reflected in the second term on the right-hand-side of equation (2). Physically this term can be evaluated as following:

$$\frac{dQ_d}{dt} = kQ = i_{d,\text{ind}} \tag{4}$$

The charge dissipation rate is directionally proportional to the total charge trapped in the liquid layer, and can be measured and evaluated as the induction current. This suggests that the device itself actually provides a way to estimate the extent of the influence of charge dissipation on the measurement. In some cases if the induction current due to residual charge dissipation, $i_{d,ind}$, is too large to be ignored, one simple method is just to wait for a short while until the dissipation current is negligibly small.

The charge measurement procedures were divided into three steps: (a), (b), and (c) as illustrated in Fig. 4. After loading the dose to the inhaler and installing the inhaler to the TSI, the charge measurement was started as follows:

Step (a): t=0, started charge measurement unit, and recorded the data for a few seconds till t=t1;
Step (b): at t=t1, introduced air flow at specified flow rate, performed TSI and electrostatic charge measurements for the formulation for 5 s, t=t2;
Step (c): at t=t2 stop air flow, continue electrostatic charge measurement for a few seconds until t=t3.

In the above three steps for charge measurement, only step (b) measured the electrostatic charge of particles via induction current method together with particle aerodynamic diameter characterization. Step (b) and (c) measured the induction current before and after particle deposition respectively, namely charge dissipation rate before and after testing. Therefore the induction current signals detected at steps (a) and (c) can be used to evaluate the magnitude of charge dissipation rate. In the current work, the dissipation currents were all very small and negligible compared to the aerosol charge signals, as can be seen in the Fig. 2.

The above observation indicated that the charge dissipation rate (measured as induction current when no particle impaction took place) immediately before and after dose testing was indeed very small. Therefore the charge dissipation was unlikely to affect the charge measurement for the current system studied, and approximation using equation (3) was valid.

Another concern is regarding the effect of the evaporation of the liquid on the charge measurement. The evaporation can be mitigated by using more viscous liquid, for example silicon oil. The extent of the liquid evaporation on charge measurement can also be evaluated using the induction current, as discussed above regarding the influence of the residual charge.

CONCLUSIONS

In the current study, a system for simultaneous measurement of electrostatic charges and particle sizes has been presented. Evaluation using the Faraday cage method showed that the accuracy in the charge measurement using the proposed system was satisfactory. Experimental results confirmed that the integration of the add-on device had no effect on the performance of TSI with regard to its FPF characterization. The developed system was applied to characterize a DPI formulation composed of Inhalac 230® and salbutamol sulphate. The measurement results indicated that salbutamol sulphate carried negative charges upon aerosolization from the lactose-based formulation that is consistent with those reported in literature. The net charges of Inhalac 230® and the un-dispersed salbutamol sulphate were positive. Charge to mass ratio results, calculated using the fine particle dose obtained from TSI measurements and charge data from the add-on device, suggested good reproducibility for the DPI system investigated.

The present integrated system provided a simple solution to simultaneously measure electrostatic charges together with particle aerodynamic diameter characterization for pulmonary drug delivery. The system can be used to characterize electrostatic charges for inhalation formulations, and to study electrostatic properties of carrier particles, inhaler materials, and other powders in general.

ACKNOWLEDGEMENT

This work was supported by the Science and Engineering Research Council of A*STAR (Agency for Science, Technology and Research), Singapore (project ICES/05-422001). The authors would also like to thank Mr. Qi Zhou, Ms Adeline Wong and Ms Syuk Yee Liow for their technical contributions during the experiments.

REFERENCES

1. S. Matsusaka, H. Umemoto, M. Nishitani, and H. Masuda. Electrostatic charge distribution of particles in gas-solids pipe flow. *J. Electrostat.* **55**:81–96 (2002). doi:10.1016/S0304-3886(01)00185-1.
2. K. W. Zhu, S. M. Rao, Q. H. Huang, C. H. Wang, S. Matsusaka, and H. Masuda. On the electrostatics of pneumatic conveying of granular materials using electrical capacitance tomography. *Chem. Eng. Sci.* **59**:3201–3213 (2004). doi:10.1016/j.ces.2004.04.019.
3. J. Yao, Y. Zhang, C. H. Wang, S. Matsusaka, and H. Masuda. Electrostatics of the granular flow in pneumatic conveying systems. *Ind. Eng. Chem. Res.* **43**:7181–7199 (2004). doi:10.1021/ie0496611.
4. A. H. Chen, H. T. Bi, and J. R. Grace. Measurement of particle charge-to-mass ratios in a gas–solids fluidized bed by a collision probe. *Powder Technol.* **135**:181–191 (2003). doi:10.1016/j.powtec.2003.08.014.
5. E. Rasanen, J. Rantanen, J. P. Mannermaa, and J. Yliruusi. The characterization of fluidization behavior using a novel multichamber microscale fluid bed. *J. Pharm. Sci.* **93**:780–791 (2004). doi:10.1002/jps.10540.

6. H. Eliasen, H. G. Kristensen, and T. Schaefer. Electrostatic charging during a melt agglomeration process. *Int. J. Pharm.* **184**:85–96 (1999). doi:10.1016/S0378-5173(99)00102-7.
7. D. A. Engers, M. N. Fricke, R. P. Storey, A. W. Newman, and K. R. Morris. Triboelectrification of pharmaceutically relevant powders during low-shear tumble blending. *J. Electrostat.* **64**:826–835 (2006). doi:10.1016/j.elstat.2006.02.003.
8. M. Murtomaa, V. Mellin, P. Harjunen, T. Lankinen, E. Laine, and V. P. Lehto. Effect of particle morphology on the triboelectrification in dry powder inhalers. *Int. J. Pharm.* **282**:107–114 (2004). doi:10.1016/j.ijpharm.2004.06.002.
9. P. R. Byron, J. Peart, and J. N. Staniforth. Aerosol electrostatics I: properties of fine powders before and after aerosolization by dry powder inhalers. *Pharm. Res.* **14**:698–705 (1997). doi:10.1023/A:1012181818244.
10. M. Murtomaa, S. Strengell, E. Laine, and A. Bailey. Measurement of electrostatic charge of an aerosol using a grid-probe. *J. Electrostat.* **58**:197–207 (2003). doi:10.1016/S0304-3886(03)00048-2.
11. P. C. L. Kwok, W. Glover, and H. K. Chan. Electrostatic charge characteristics of aerosol produced from metered dose inhalers. *J. Pharm. Sci.* **94**:2789–2799 (2005). doi:10.1002/jps.20395.
12. K. W. Zhu, R. B. H Tan, F. X. Chen, K. H. Ong, and P. W. S. Heng. Influence of particle wall adhesion on particle electrification in mixers. *Int. J. Pharm.* **328**:22–34 (2007). doi:10.1016/j.ijpharm.2006.07.041.
13. K. W. Zhu, R. B. H. Tan, W. K. Ng, S. C. Shen, Q. Zhou, and P. W. S. Heng. Analysis of the influence of relative humidity on the moisture sorption of particles and the aerosolization process in dry powder inhaler. *J. Aerosol Sci.* **39**:510–524 (2008). doi:10.1016/j.jaerosci.2008.02.003.
14. P. M. Young, A. Sung, D. Traini, P. C. L. Kwok, H. Chiou, and H. K. Chan. Influence of humidity on the electrostatic charge and aerosol performance of dry powder inhaler carrier based systems. *Pharm. Res.* **24**:963–970 (2007). doi:10.1007/s11095-006-9218-8.
15. P. C. L. Kwok, and H. K. Chan. Effect of relative humidity on the electrostatic charge properties of dry powder inhaler aerosols. *Pharm. Res.* **25**:277–288 (2007). doi:10.1007/s11095-007-9377-2.
16. A. G. Bailey, A. H. Hashish, and T. J. Williams. Drug delivery by inhalation of charged particles. *J. Electrostat.* **44**:3–10 (1998). doi:10.1016/S0304-3886(98)00017-5.
17. W. I. Li, M. Perzl, J. Heyder, R. Langer, J. D. Brain, K. H. Englmeier, R. W. Niven, and D. A. Edwards. Aerodynamics and aerosol particle deaggregation phenomena in model oral–pharyngeal cavities. *J. Aerosol Sci.* **27**:1269–1286 (1996). doi:10.1016/0021-8502(96)00046-8.
18. J. P. Mitchell, D. P. Coppolo, and M. W. Nagel. Electrostatics and inhaled medications: influence on delivery via pressurized metered-dose inhalers and add-on devices. *Respir. Care*. **52**:283–300 (2007).
19. V. A. Philip, R. C. Mehta, M. K. Mazumder, and P. P. DeLuca. Effect of surface treatment on respirable fractions of PLGA microspheres formulated for dry powder inhalers. *Int. J. Pharm.* **151**:165–174 (1997). doi:10.1016/S0378-5173(96)04879-X.
20. D. Traini, P. M. Young, M. Jones, S. Edge, and R. Price. Comparative study of erythritol and lactose monohydrate as carriers for inhalation: atomic force microscopy and *in vitro* correlation. *Eur. J. Pharm. Sci.* **27**:243–251 (2006). doi:10.1016/j.ejps.2005.10.005.
21. W. Glover, and H. K. Chan. Electrostatic charge characterization of pharmaceutical aerosols using electrical low-pressure impaction (ELPI). *J. Aerosol Sci.* **35**:755–764 (2004). doi:10.1016/j.jaerosci.2003.12.003.
22. J. C. Dubus, C. Guillot, and M. Badier. Electrostatic charge on spacer devices and salbutamol response in young children. *Int. J. Pharm.* **261**:159–164 (2003). doi:10.1016/S0378-5173(03)00314-4.
23. B. Y. Shekunov, P. Chattopadhyay, H. H. Y. Tong, and A. H. L. Chow. Particle size analysis in pharmaceutics: principles, methods and applications. *Pharm. Res.* **24**:203–227 (2007). doi:10.1007/s11095-006-9146-7.
24. J. P. Mitchell, and M. W. Nagel. Particle size analysis of aerosols from medicinal inhalers. *KONA*. **22**:32–65 (2004).
25. E. O. Knutson, and K. T. Whitby. Aerosol classification by electric mobility: apparatus, theory and applications. *J. Aerosol Sci.* **6**:443–451 (1975). doi:10.1016/0021-8502(75)90060-9.
26. W. C. Hinds. *Aerosol Technology, Properties, Behaviour and Measurements of Airborne Particles*. Wiley, New York, 1982.
27. P. V. Wells, and R. H. Gerke. An oscillation method for measuring size of ultramicroscopic particles. *J. Amer. Chem. Soc.* **41**:312–329 (1919). doi:10.1021/ja01460a004.
28. N. A. Fuchs. *The Mechanics of Aerosols*. Dover, New York, 1964.
29. J. Keshinen, K. Pietarinen, and M. Lehtimaki. Electrical low pressure impactor. *J. Aerosol Sci.* **23**:353–360 (1992). doi:10.1016/0021-8502(92)90004-F.
30. M. J. Telko, J. Kujanpaa, and A. J. Hickey. Investigation of triboelectric charging in dry powder inhalers using electrical low pressure impactor (ELPI^{TM}). *Int. J. Pharm.* **336**:352–360 (2007). doi:10.1016/j.ijpharm.2006.12.018.
31. P. C. L. Kwok, T. Noakes, and H. K. Chan. Effect of moisture on the electrostatic charge properties of metered dose inhaler aerosols. *J. Aerosol Sci.* **39**:211–226 (2008). doi:10.1016/j.jaerosci.2007.11.004.
32. J. P. Mitchell, and M. W. Nagel. Cascade impactors for the size characterization of aerosols from medical inhalers: their use and limitation. *J. Aerosol Med.* **16**:341–376 (2003). doi:10.1089/089426803772455622.
33. A. Elajnaf, P. Carter, and G. Rowley. Electrostatic characterisation of inhaled powders: effect of contact surface and relative humidity. *Eur. J. Pharm. Sci.* **29**:375–384 (2006). doi:10.1016/j.ejps.2006.07.006.
34. S. Matsusaka, H. Fukuda, Y. Sakura, H. Masuda, and M. Ghadiri. Analysis of pulsating electric signals generated in gas–solids pipe flow. *Chem. Eng. Sci.* **63**:1353–1360 (2008). doi:10.1016/j.ces.2007.07.010.